*Original Russian Text:* Ignatova A.V., Kudryavtsev O.A., Sapozhnikov S.B. Experimental investigation and numerical modeling of elastic properties and strength of porous ceramics. *PNRPU Mechanics Bulletin*, 2015, no. 4. pp. 121-137. DOI: 10.15593/perm.mech/2015.4.08

**PNRPU MECHANICS BULLETIN**

**№ 1-2, 2018**

http://vestnik.pstu.ru/mechanics/about/inf/

DOI: 10.15593/perm.mech/eng.2018.1.08
UDC 539.3 + 539.422 + 666.3:539.3

# EXPERIMENTAL INVESTIGATION AND NUMERICAL MODELING OF ELASTIC PROPERTIES AND STRENGTH OF POROUS CERAMICS

**A.V. Ignatova, O.A. Kudryavtsev, S.B. Sapozhnikov**

South Ural State University, Chelyabinsk, Russian Federation

ARTICLE INFO

Received: 22.06.2015
Accepted: 13.10.2015
Published: 30.06.2018

*Keywords:*

advanced ceramics, porosity, strength, elastic module, Poisson ratio, finite element analysis

ABSTRACT

Advanced ceramics are widely used in responsible structures that work at conditions of high temperature changes, strong electrical fields and impact loads. Sintered ceramics are usually porous which affects their strength and elastic properties. In the first part of this work the results of experimental and numerical strength investigations of hot-pressed alumina ceramic are presented. The disk-shaped specimens with different porosity (4-23 %) were subjected to Piston-on-Ring bending test up to failure. Ultimate tensile strength is varied in the range of 180…490 MPa. Finite element method was used for stress state analysis of ceramic disk during bending test. Elastic properties of porous ceramic for numerical simulations were determined by using the known approximation of dependences “property – porosity” and some experimental data. In the second part of this work three-dimensional numerical micromodel was created in ANSYS. This model is a cube with set pores up to 160 of spherical forms. The diameter of sphere is given by Weibull distribution with mean value $m$ = 0.139 μm and standard deviation $s$ = 0.075 μm (defined by SEM analysis of fracture surfaces). Scale parameter λ = 0.164 μm and shape parameter $k$ = 1.919 of the Weibull distribution was determined by the least squares method. The authors generated three to six models with a random distribution of pores for each average porosity; and analyzed stress state under axial tension for each case. The maximum normal stress, stress concentration factor, elastic modulus and Poisson's ratios are dependent on the average porosity. The values of the tensile strength were defined for different porosity according to the Rankine criterion (maximum normal stress criterion). These values are in a good agreement with the experimental results before porosity of 15 %.



© **Anastasia V. Ignatova** – Engineer, e-mail: ignatovaav@susu.ac.ru

**Oleg A. Kudryavtsev** – Ph. D. student, e-mail: kudriavtcevoa@susu.ac.ru

**Sergei B. Sapozhnikov** – Doctor of Technical Sciences, Professor, e-mail: ssb@susu.ac.ru

## Introduction

Ceramic materials have a number of unique properties, such as high hardness, wear resistance, low density, high strength under compression and etc. They are widely used in industies, in airspace, in production of protective structures [1, 2]. At the same time, a low strength of ceramics under tension (approximately by an order of magnitude lower, than the strength under compression) and a brittle nature of ceramics significantly limits their application. The ultimate strength under tension is one of major parameters, determining the quality of ceramics [3] associated with the presence of defects in its structure (pores and microcracks).

There are several approaches which consider deformation and fracture of brittle materials. When solving the problems related to the interaction of ceramics and high-velocity projectiles (first of all, in the frame of protective structures), the models of a persistently damaged homogeneous material [4] and its modifications are most popular now. The example of using this model can be found in [6-12]. However these models require determining a significant number of parameters, which is quite a sophisticated problem, and requires a great number of experiments, such as Edge-On-Impact (EOI) or Depth-Of-Penetration (DOP) tests.

In order to take account of the stochastic peculiarities of deformation and fracture of ceramic materials, a good compliance with the experimental data is found, if one uses cohesive elements in calculations (cohesive/volumetric finite element – CVFE) [13-16]. In [17, 18] the authors directly considered the microstructure of the ceramic material by obtaining a qualitative and quantitative conformity with the experimental data under static and dynamic loadings. Apart from that, in [19, 20] the method of cohesive elements was used for modelling fracture and distribution of cracks in ceramics at a high-velocity impact. However, the justification and selection of parameters of cohesive elements is still a subject matter. It is also worth mentioning, that the "cohesive" approach requires considerable computational efforts, associated with an increase of dimensionality of the solved problems, compared to the traditional approach in LS-DYNA, based on the analysis of eliminating damaged elements (death-of-element analysis).

It is important to note that it is necessary to consider the size and form of defects, their quantity and bulk arrangement in order to predict the fracture mechanisms of porous ceramics [21-24]. The authors of the mentioned works modelled the material microstructure by considering the stochastic destribution of pores in a two- and three dimensional setting. According to their results, we can conclude that the availability of several neighboring defects with different sizes leads to an abrupt decrease of a material's strength.

This work presents the computational and experimental evaluation of the ultimate strength under tension by the example of $Al_2O_3$ceramics with different densities. For this purpose the Piston-on-Ring bending test of discs were made. Then we compared the ultimate strength and elastic characteristics of ceramics with different densities to the results gained by using the finite element method in the models with a random destribution of spherical pores, and the relations "elastic module-porosity", available in the literature.

## 1. Experimental Part

### 1.1. Production of Specimens

To press ceramics, we used the nanopowder of aluminium oxide ($Al_2O_3$), obtained with the method of the electrofilter condensation of vapors. Fig. 1 shows the microscopic structure of the powder material. The average size of the agglomerates of nanoparticles is 220 nm.

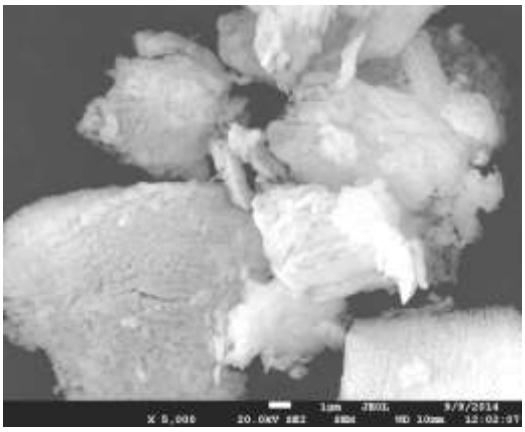

Fig. 1. The initial powder $Al_2O_3$ (agglomerates)

For the production of samples, a hot pressing machine HP20-4560-20 from Thermal Technology LLC was used. The specimen of a powder weighing 5.95 ± 0.05 g prepared for compacting was filled into a matrix mounted on the lower punch and pre-compressed with an upper punch with a force of 75 kg. Punches, matrix and thermal insulation were made of graphite, the diameter of the resulting billet was 25.4 mm. Then the following program of roasting and pressing was launched:

– the evacuation of air from the furnace by means of a fork-vacuum pump to a residual pressure in the chamber of ~ 0.2 millimeter of mercury;

– heating to 1200 ° C at a speed of 20 °C/min with a constant pressing force F (four load levels F were used to produce samples of different porosity, i.e. 1000; 1500, 2000 and 2500 kg);

– exposure at 1200 °C and constant pressing force *F* for 20 minutes;

– unloading and cooling to room temperature together with the furnace for 3 hours.

By varying the pressing load, it became possible to obtain the specimens of ceramics with different porosities; the characteristics of the specimens are shown in Table 1.

Seven samples were produced at each load level. The density of a conventionally non-porous material was assumed to be equal to$_0$ = 3.99 g/cm$^3$ [2].

Table 1

Characteristics of hot-pressed specimens

| Group of speci-mens | Pressing load $F$, kg | Mass, g | Height, mm | Density ρ, g/cm $^3$ | Specific average density $\rho/\rho_0$ |
|---|---|---|---|---|---|
| 1 | 1000 | 5.93±0.03 | 3.83±0.05 | 3.06±0.04 | 0.77 |
| 2 | 1500 | 5.94±0.01 | 3.32±0.04 | 3.53±0.04 | 0.89 |
| 3 | 2000 | 5.94±0.02 | 3.12±0.03 | 3.75±0.03 | 0.94 |
| 4 | 2500 | 5.92±0.02 | 3.05±0.02 | 3.82±0.01 | 0.96 |

### 1.2. Determination of the Elasticity Constants

To evaluate the ultimate strength in the axisymmetric bending of the disk specimens, there are no simple analytical relationships connecting the fracture load with the sizes and mechanical properties of the material; therefore, we used the finite element method, in which for the analysis of the stress state, it is necessary to introduce the values of the elasticity constants for each level of ceramic density (see point 2.3 below). The results of the analysis of the literature sources for the determination of these constants are shown below.

In [25] the dependences of the shear modulus G and the volumetric modulus of elasticity K for α-$Al_2O_3$ ceramics on porosity, as an isotropic elastic material in the range of porosity of 0-40 % are proposed:

$$K = K_0 \cdot \exp\left(-3.96\frac{P}{1-P}\right), \quad (1)$$

$$G = G_0 \cdot \exp\left(-1.617\frac{P}{1-P}\right), \quad (2)$$

where $P$ is porosity (dimensionless value). For the nonporous material, the elasticity constants $K_0$ и $G_0$ (Table 2) were adapted from the work in [2].

According to formulae (1) and (2) for each level of a mean relative density (porosity) of the specimens, the shear moduli were calculated, as well as the volumetric modulus of elasticity, given in Table 3. The values of the Poisson's coefficients and the elastic moduli were calculated using the known formulas of the theory of isotropic elasticity.

From Table 3 it follows that the Poisson's ratio reaches a value of 0.04 with a porosity of 23 %, and it becomes negative with a further increase in porosity. At the moment there is no universally accepted relation "Poisson's ratio – porosity" for different densities of material [26]. The experimental studies for α-$Al_2O_3$ in [26, 27] showed that the Poisson's ratio slightly decreases, when the porosity increases from 0 to 25 % (Table 4). These data (interpolation) were used in the present work.

Table 2

Elasticity constants for nonporous α-$Al_2O_3$

| Elastic module $E_0$, GPa | The volumetric modulus of elasticity $K_0$, GPa | Shear module $G_0$, GPa | Poisson ratio $\nu_0$ |
|---|---|---|---|
| 402 | 251 | 163 | 0.233 |

Table 3

Elastic constants for materials with different porosity

| Group of specimens | Mean relative density $\rho/\rho_0$ | Elastic module $E$, GPa | The volumetric elastic module $K$, GPa | Shear module $G$, GPa | Poisson's ratio ν |
|---|---|---|---|---|---|
| 1 | 0.77 | 214 | 78 | 103 | 0.04 |
| 2 | 0.89 | 317 | 155 | 136 | 0.16 |
| 3 | 0.94 | 359 | 197 | 150 | 0.195 |
| 4 | 0.96 | 376 | 216 | 156 | 0.208 |

To determine the dependence of the elastic modulus on the material mass density $E(P)$ for porous ceramics, a set of relations is proposed [27-31]. Let us note that the reliable experimental data on the elastic modulus of aluminum oxide are obtained by ultrasonic methods with a porosity of not more than 40 %.

The semi-linear dependence of $E(P)$, proposed in [31], is applicable up to a porosity of not more than 0.3, since with a greater porosity the function begins to increase, which does not correspond to the experimental data. Other relations (Fig. 2) have a similar character. By summarizing the analysis results of the published sources, the authors of this article concluded that in numerical calculations the relation in [29] should be used:

$$E = E_0 \cdot (1-P) \cdot \left(1-\frac{P}{0.684}\right), \quad (3)$$

which give average results between the relations given in [25] and [27].

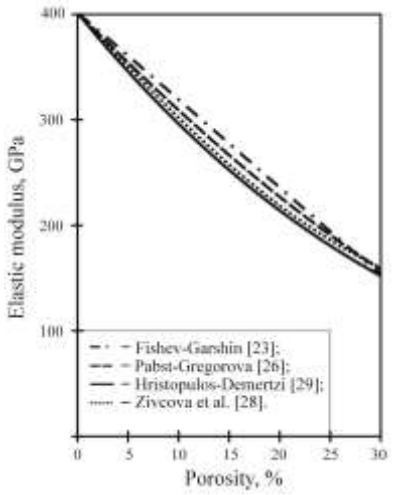


Fig. 2. Relations describing the change of the elastic modulus α-$Al_2O_3$ for different porosity

Table 4 contains the values of the elastic modulus at fixed conditions of porosity, obtained according to the relation in (3).

### 1.3. Testing Before Fracture and Analysis of Strength

To determine the material ultimate strength of the ceramic specimens, testing up to failure were carried out. The tests were carried according to the scheme of the Piston-on-Ring bending test (Fig. 3). The method is described in [32]. With this loading, a biaxial tension occurs in the center of the lower surface of the specimen, causing the development of radial cracks. The value of the maximum tensile stress (the first principal stress is the criterion of failure) can be used with the accuracy sufficient for engineering applications in evaluating the ultimate strength under uniaxial tension. The parameters of the supports were as follows: the diameter of the top was 5 mm; the diameter of the supporting surface aws 19.0 mm. Fig. 4 shows the specimens after testing.

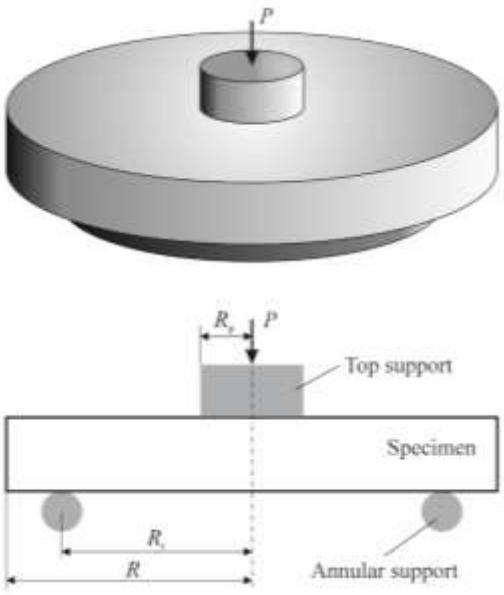


Fig. 3. The cheme of the specimen on a ring support

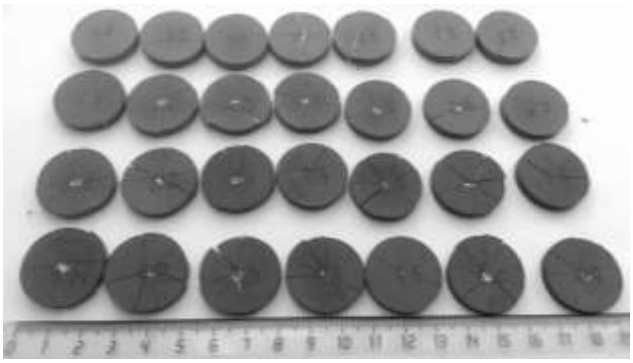

Fig. 4. The specimens after testing according to the scheme of the Piston-on-Ring bending test

The stress-strain state of the specimen and the value of the maximum tensile stress were determined in the ANSYS package, by implementing the finite element method (FEM). A dry friction with a coefficient of 0.1 was set at the contact point between the experimental setup and the specimen. The material was considered isotropic and linearly elastic. In calculating the FEM from symmetry considerations, only ¼ of the model was studied to save computational resources. As an example, Fig. 5 presents the computational scheme with the FE mesh; and the distribution of the first principal stresses over the thickness of the sample is shown for bending on a ring support. For groups with different densities, similar computations were made.

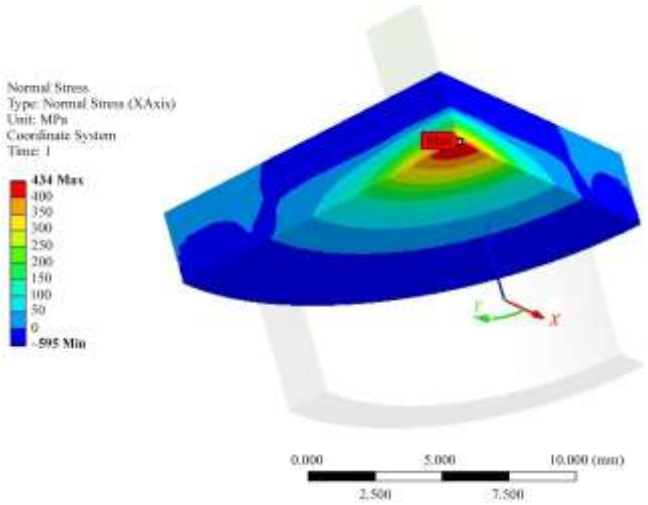


Fig. 5. Destribution of first principal stresses across the width of the specimen with the porosity of 4 %

The obtained computational values of the ultimate strength of specimens with different porosity is given in Table 4.

Table 4

Elastic constants and obtained values of the ultimate strength for ceramics used for the calculations

| A group of specimens | Mean relative density $\rho/\rho_0$ | Poro-sity $P$ | Elastic modulus $E$, GPa | Poisson's ratio ν | Mean value of the failure load $F$, H | Mean value of the ultimate strength $\sigma_B$, MPa |
|---|---|---|---|---|---|---|
| 1 | 0.77 | 0.23 | 205 | 0.199 | 2455 | 182 |
| 2 | 0.89 | 0.11 | 300 | 0.222 | 3115 | 299 |
| 3 | 0.94 | 0.06 | 345 | 0.229 | 3521 | 377 |
| 4 | 0.96 | 0.04 | 363 | 0.230 | 3902 | 429 |

When describing the dependence of the material strength of the ceramic samples under tension/compression on porosity, a good agreement with the experimental data belongs to the relation in [33]:

$$\sigma = \sigma_0 \cdot \exp(-n \cdot P), \quad (4)$$

where $\sigma_0$ is the ultimate strength of the nonporous material, $P$ is porosity (volume fraction of pores), n is the empirical constant.

Fig. 6 shows the experimental values of the strength limits in the porosity function of the studied ceramics and the approximating curve (4), in which the parameters $\sigma_0 = 510$ MPa, $n = 4.63$ are determined using the least squares method.

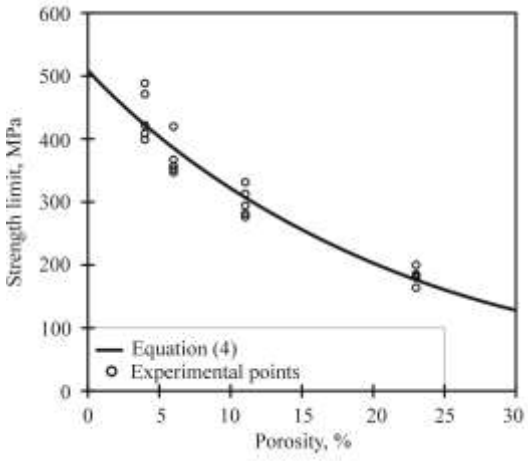


Fig. 6. The dependence of the material utlimate strength of ceramic specimens on porosity

It is indicative that for a high-density ceramics a slight increase in porosity (by 5-10 %) leads to a sharp decrease in the ultimate strength (by 25-30 %).

### 1.4. Studying the Microstructure of Ceramics

The analysis of the ceramics' microstructure was made based on the images of the surface of fracture, using the scanning electron microscope (Jeol JEM 2100). Pores are clearly seen on the surface of the break in the ceramic specimens, their sizes are in the range of 15-380 nm. The statistical processing of pore sizes at the images showed that ceramics of different porosities have a close pore size distribution and a different number of pores (Fig. 7, *a*-*d*).

Based on the sampled values of the pore diameters, an empirical distribution function is constructed using the standard formula

$$F^*(x) = \frac{n_x}{n}, \tag{5}$$

where $n_x$ is the number of pores with a diameter less than $x$; $n$ is the sample size [34, 35]. Further, this distribution function was approximated by the Weibull distribution

$$F(x) = 1 - \exp\left(-\left(\frac{x}{\lambda}\right)^k\right), \tag{6}$$

here $\lambda$ is the scale factor**,** $k$ is the shape parameter**.** The scale factor $\lambda = 0.164$ micron and the parameter of shape $k = 1.919$ were determined by the the least square method, when comparing the empirical and theoretical laws of distribution. According to formulas given in [35], for the Weibull distribution we obtained the mathematical expectation $m = 0{,}139$ μm and mean-square deviation $s = 0.075$ μm. Figure 8 shows the empirical (more than 300 measurements) distribution $F(x)$ of pore diameter values and the theoretical Weibull distribution.

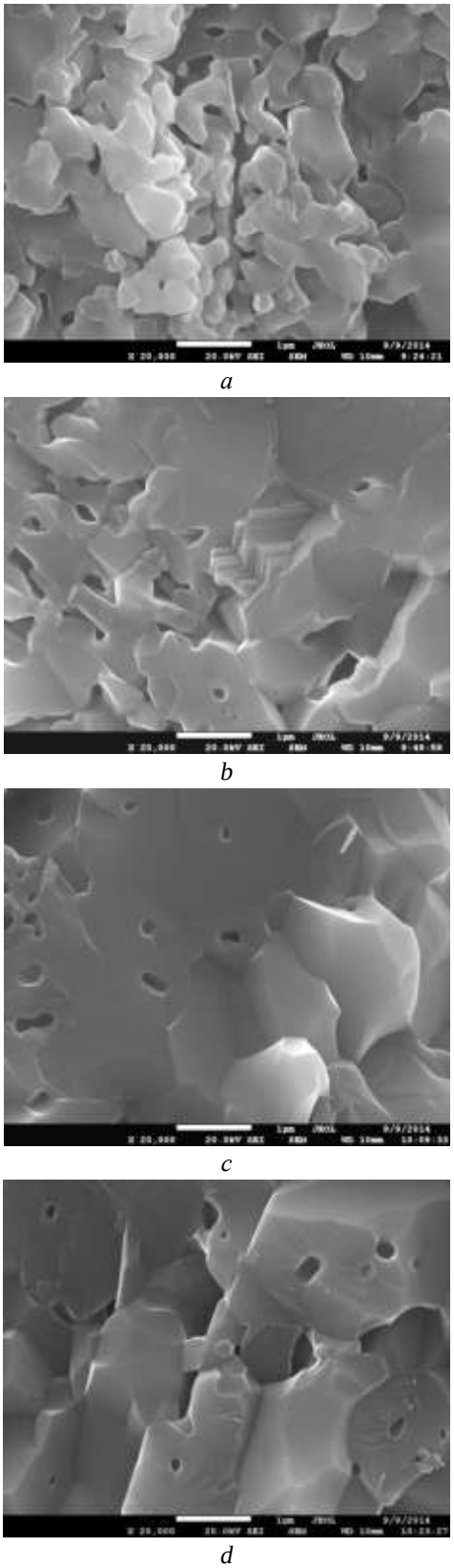

*a*

*b*

*c*

*d*

Fig. 7. The surface of the break in ceramic specimens with different porosities (*a* – 0.24; *b* – 0.11; *c* – 0.06; *d* – 0.04)

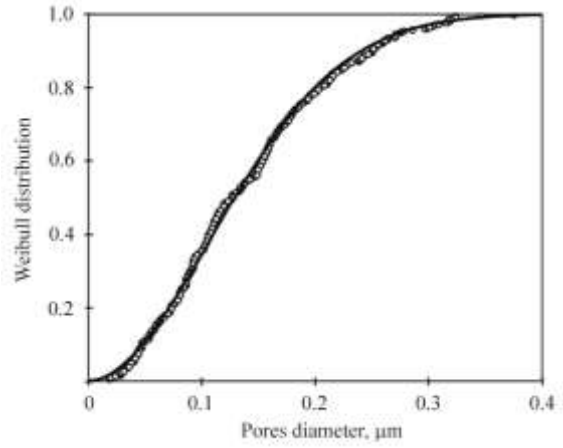


Fig. 8. Weibull distribution of pores diameter

## 2. Computational Part

To predict the mechanical characteristics (ultimate strength, elastic modulus, Poisson's ratio) of porous ceramics, a numerical model with multiple pores was developed. Assumptions were made about the isotropic elasticity and brittleness of ceramics; all pores have a spherical shape, the pore center coordinates are given by a random number generator with a uniform distribution density. The diameter of pores was set according to the Weibull distribution law (point 2.4). All the parameters (pore center coordinates and diameter) were recorded in an Excel file and then in the SolidWorks package three-dimensional models were constructed in the form of a cube, Fig. 9, containing up to 160 pores. The analysis of the model's stress state was made in ANSYS using the finite elements method. The strength of the porous ceramic was evaluated by the applied average tensile stress at which the maximum normal stress is equal to the ultimate strength of the defect-free ceramic.

The general view of the element (100×100×100 mm) with the finite element mesh is given in Fig. 9, the size of the face of the finite element (the second-order tetrahedron) is equal to ~8 mm.

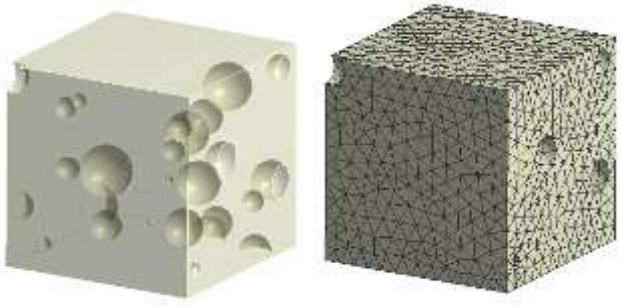

Fig. 9. Model (transparent) and finite element mesh for porosity of 6 %

Figure 10 shows the results of calculating the first principal stresses with the applied uniaxial tensile stress of 1.0 MPa.

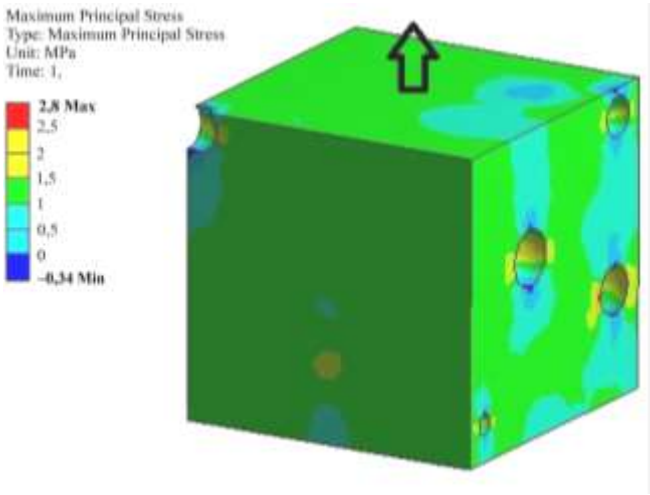


Fig. 10. Destribution of first principal stresses in the cell under uniaxial tension (the porosity of 6 %)

The concentration factor was calculated based on the formula $\alpha = \dfrac{\max(\sigma_1)}{\sigma_{nom}}$, where $\max(\sigma_1)$ is the maximum value of the first primary stress, $\sigma_{nom}$ = 1,0 MPa is the applied nominal stress.

The ultimate strength of ceramics $\sigma(P)$ *c*an be calculated using the following relation

$$\sigma(P) = \frac{\sigma_*}{\alpha(P)} \qquad (7)$$

where $\sigma_*$ is the theoretical strength of the pore-free ceramics (in this case it is the empirically determined parameter). Fig. 11 shows the calculated values of the ultimate strength (points), when $\sigma_*$ = 1300 MPa and the empirical relation is in (4).

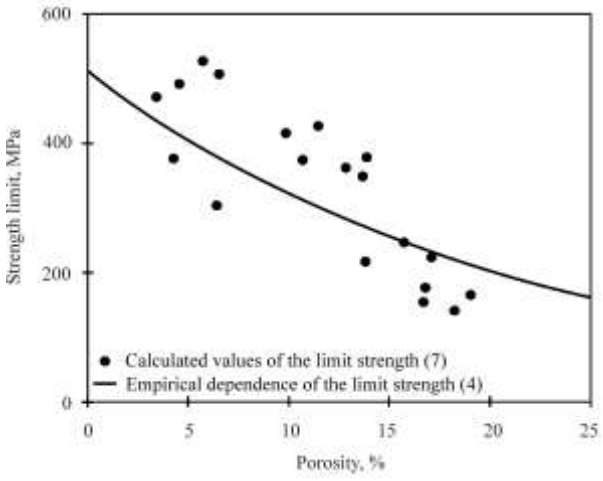


Fig. 11. The dependence of the material utlimate strength of ceramic specimens on porosity

The calculated (FEM) values of elestic moduli and Poisson's ratios depending on the ceramics porosity are shown in Fig. 12 with dots, and the respective empirical relations are shown with lines.

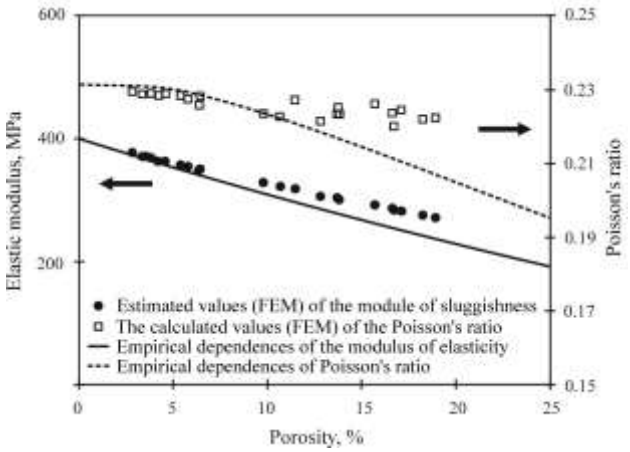


Fig. 12. The dependences of the elastic modulus and Poisson's ratio for ceramics on porosity

According to the data presented, it can be concluded that the model developed with a random pore distribution is in a satisfactory agreement with the experimental data: the error in determining all the mechanical characteristics does not exceed 10 % to a porosity of 15 %.

## Conclusions

The technology of hot sintering in vacuum of nanopowder of aluminum oxide in vacuum is tested, and disc-shaped specimens with the porosity of 4, 6, 11 and 23 % are produced. The bending test of the specimens proved that the ultimate strength varies in the range of 180…490 MPa.

The analysis (scanning electron microscope) of the break surfaces of the specimens with different porosity showed that the ceramics has rounded pores with the sizes of 15…380 μm, and the distribution function is the same in the considered range of porosities, and can be approximated with the two-parameter Weibull law with the scale factor $\lambda = 0.164$ μm and parameter of shape $k = 1.919$.

A three-dimensional numerical model with a random distribution of pores in the volume of an isotropic elastic brittle material has been developed. This model made it possible to obtain the dependencies of the elastic modulus, the Poisson's ratio of ceramics, and also the ultimate strength on the porosity of the material, having only one empirical parameter, i.e. the ultimate tensile strength of a defect-free ceramic.

The developed model and the results obtained on its basis can be used in engineering.

The research was made at South Ural State University (a national research university) supported by the The Russian Scientific Foundation (Project №14-19-00327). All the experiments were made using the facilities of the Research and Educational Center NANOTECHNOLOGIES of South Ural State University.

## References

1. Hazell P.J. Ceramic Armour: Design and Defeat Mechanisms. Canberra, Argos Press, 2006, 168 p.

2. Carter C.B., Norton M.G. Ceramic materials: Science and Engineering. 2nd ed. New York, Springer, 2007, 716 p.

3. Danzer R. On the relationship between ceramic strength and the requirements for mechanical design. *Journal of the European Ceramic Society*, 2014, vol. 34, no. 15, pp. 3435-3460.

4. Johnson G.R., Holmquist T.J. A computational constitutive model for brittle materials subjected to large strains, high strain rates, and high pressures. *Proceedings of EXPLOMET Conference (San Diego, California)*. New York: Marcel Dekker Inc., 1992, pp. 1075-1081.

5. Johnson G.R. Numerical algorithms and material models for high-velocity impact computations. *International Journal of Impact Engineering*, 2011, vol. 38, pp. 456-472.

6. Ong C.W., Boey C.W., Hixson R.S., Sinibaldi J.O. Advanced layered personnel armor. *International Journal of Impact Engineering*, 2011, vol. 38, pp. 369-383.

7. Bürger D., de Faria A.R., de Almeida S.F.M., de Melo F.C.L., Donadon M.V. Ballistic impact simulation of an armour-piercing projectile on hybrid ceramic/fiber reinforced composite armours. *International Journal of Impact Engineering*, 2012, vol. 43, pp. 63-77.

8. Feli S., Asgari M.R. Finite element simulation of ceramic/composite armor under ballistic impact. *Composites: Part B*, 2011, vol. 42, pp. 771-780.

9. Prakash A., Rajasankar J., Anandavalli N., Verma M., Iyer N.R. Influence of adhesive thickness on high velocity impact performance of ceramic/metal composite targets. *International Journal of Adhesion & Adhesives*, 2013, vol. 41, pp. 186-197.

10. Tan P. Numerical simulation of the ballistic protection performance of a laminated armor system with pre-existing debonding/delamination. *Composites: Part B*, 2014, vol. 59, pp. 50-59.

11. Holmquist T.J., Johnson G.R. Response of boron carbide subjected to high-velocity impact. *International Journal of Impact Engineering*, 2008, vol. 35, pp. 742-752.

12. Deshpande V.S., Evans A.G. Inelastic deformation and energy dissipation in ceramics: A mechanism-based constitutive model. *Journal of the Mechanics and Physics of Solids*, 2008, vol. 56, pp. 3077-3100.

13. Zhou F., Molinari J.F. Stochastic fracture of ceramics under dynamic tensile loading. *International Journal of Solids and Structures*, 2004, vol. 41, pp. 6573-6596.

14. Yu R.C., Ruiz G., Pandolfi A. Numerical investigation on the dynamic behavior of advanced ceramics. *Engineering Fracture Mechanics*, 2004, vol. 71, pp. 897-911.

15. Maiti S., Rangaswamy K., Geubelle P.H. Mesoscale analysis of dynamic fragmentation of ceramics under tension. *Acta Materialia*, 2005, vol. 53, pp. 823-834.

16. Levy S., Molinari J.F. Dynamic fragmentation of ceramics, signature of defects and scaling of fragment sizes. *Journal of the Mechanics and Physics of Solids*, 2010, vol. 58, pp. 12-26.

17. Clayton J.D., Kraft R.H., Leavy R.B. Mesoscale modeling of nonlinear elasticity and fracture in ceramic polycrystals under dynamic shear and compression. *International Journal of Solids and Structures*, 2012, vol. 49, pp. 2686-2702.

18. Wang D., Zhao J., Zhou Y.H., Chen X.X., Li A.H., Gong Z.C. Extended finite element modeling of crack propagation in ceramic tool materials by considering the microstructural

features. *Computational Materials Science*, 2013, vol. 77, pp. 236-244.

19. Radovitzky R., Seagraves A., Tupek M., Noels L. A scalable 3D fracture and fragmentation algorithm based on a hybrid, discontinuous Galerkin, cohesive element method. *Computer Methods in Applied Mechanics and Engineering*, 2011, vol. 200, pp. 326-344.

20. Lee M., Kim E.Y., Yoo Y.H. Simulation of high speed impact into ceramic composite systems using cohesive-law fracture model. *International Journal of Impact Engineering*, 2008, vol. 35, pp. 1636-1641.

21. Konovalenko Ig.S., Smolin A.Yu., Konovalenko Iv.S., Promakhov V.V., Psakhie S.G. Komp'iuternoe issledovanie zavisimosti mekhanicheskikh svoistv khrupkogo materiala ot partsial'noi kontsentratsii por raznogo razmera v ego strukture [Computer-based study of the dependence of mechanical properties of brittle porous material on the partial concentration of pores of different size]. *Tomsk State University Journal of Mathematics and Mechanics*, 2013, no. 6 (26), pp. 79-87.

22. Smolin I.Yu., Eremin M.O., Makarov P.V., Buyakova S.P., Kul'kov S.N., Evtushenko E.P. Chislennoe modelirovanie mekhanicheskogo povedeniia model'nykh khrupkikh poristykh materialov na mezourovne [Numerical modelling of mechanical behaviour of model brittle porous materials at the mesoscale]. *Tomsk State University Journal of Mathematics and Mechanics*, 2013, no. 5 (25), pp. 78-90.

23. Slutsker A.I., Sinani A.B., Betekhtin V.I., Kozhushko A.A., Kadomtsev A.G., Ordanyan S.S. Influence of microporosity on the strength properties of SiC ceramic materials. *Physics of the Solid State*, 2008, vol. 50, no. 8, pp. 1450-1457.

24. Kadomtsev A.G., Slutsker A.I., Sinani A.B., Betekhtin Vl.I., Damaskinskaya E.E. Lokal'nye razrushaiushchie napriazheniia i tverdost' mikroporistoi SiC-keramiki [Local breaking stresses and hardness of microporous SiC-ceramics]. *Journal "Tambov University Review. Series: Natural and Technical Sciences"*, 2013, vol. 18, no. 4, pp. 1533-1534.

25. Garshin A.P., Gropoyanov V.M., Zaytsev G.P., Semenov S.S. Keramika dlia mashinostroeniia [Ceramics for engineering]. Moscow: Nauchtekhlitizdat, 2003, 384 p.

26. Asmani M., Kermel C., Leriche A., Ourak M. Influence of porosity on Young's modulus and Poisson's ratio in alumina ceramics. *Journal of the European Ceramic Society*, 2001, vol. 21, pp. 1081-1086.

27. Zivcova Z., Cerny M., Pabst W., Gregorova E. Elastic properties of porous oxide ceramics prepared using starch as a pore-forming agent. *Journal of the European Ceramic Society*, 2009, vol. 29, pp. 2765-2771.

28. Phani K.K., Sanyal D. The relations between the shear modulus, the bulk modulus and Young's modulus for porous isotropic ceramic materials. *Materials Science and Engineering A*, 2008, vol. 490, pp. 305-312.

29. Pabst W., Gregorova E., Ticha G. Elasticity of porous ceramics – A critical study of modulus – porosity relations. *Journal of the European Ceramic Society*, 2006, vol. 26, pp. 1085-1097.

30. Dorey R.A., Yeomans J.A., Smith P.A. Effect of pore clustering on the mechanical properties of ceramics. *Journal of the European Ceramic Society*, 2002, vol. 22, pp. 403-409.

31. Hristopulos D.T., Demertzi M. A semi-analytical equation for the Young's modulus of isotropic ceramic materials. *Journal of the European Ceramic Society*, 2008, vol. 28, pp. 1111-1120.

32. Huang C.W., Hsueh C.H. Piston-on-three-ball versus piston-on-ring in evaluating the biaxial strength of dental ceramics. *Dental materials*, 2011, vol. 27, pp. 117-123.

33. Duckworth W. Discussion of Ryshkewitch paper by Winston Duckworth. *Journal of the American Ceramic Society*, 1953, vol. 36, pp. 68-69.

34. Gmurman V.E. Teoriia veroiatnosti i matematicheskaia statistika. Moscow, Vysshaia shkola, 2003, 479 p.

35. Stepnov M.N. Statisticheskie metody obrabotki rezul'tatov mekhanicheskikh ispytanii: spravochnik. Moscow, Mashinostroenie, 1985, 232 p.